Available online at www.sciencedirect.com

SciVerse ScienceDirect

Ceramics International 39 (2013) 2803–2810

CERAMICS INTERNATIONAL

www.elsevier.com/locate/ceramint

Synthesis of large-scale uniform mulberry-like ZnO particles with microwave hydrothermal method and its antibacterial property

Jianzhong Ma[a,c,*], Junli Liu[b,c], Yan Bao[a,c], Zhenfeng Zhu[b,c], Xiaofeng Wang[b,c], Jing Zhang[d]

[a]College of Resources and Environment, Shaanxi University of Science and Technology, Xi'an 710021,PR China
[b]College of Materials Science and Engineering, Shaanxi University of Science and Technology, Xi'an 710021,PR China
[c]Key Laboratory for Light Chemical Additives and Technology of Ministry of Education, Shaanxi University of Science & Technology, Xi'an 710021, PR China
[d]College of Foreign Languages and Communications, Shaanxi University of Science and Technology, Xi'an 710021,PR China

Received 25 August 2012; received in revised form 14 September 2012; accepted 14 September 2012
Available online 23 September 2012

Abstract

Large-scale uniform mulberry-like ZnO particles were successfully synthesized via a fast and simple microwave hydrothermal method. The formation mechanism of mulberry-like ZnO particles was investigated by adding different types of alkalis and different amounts of triethanolamine (TEA). Transmission electron microscopy (TEM), scanning electron microscopy (SEM) and X-ray diffraction (XRD) were used to observe the morphology and crystal structure of the obtained ZnO. The results revealed that the as-prepared ZnO products had an average diameter of about 150 nm and polycrystalline wurtzite structure. The existence of TEA was vital for the formation of nanoparticle-assembled mulberry-like ZnO particles. These mulberry-like ZnO particles exhibited stronger antibacterial effects on *Candida albicans* than did sheet-like and flower-like ZnO.
© 2012 Elsevier Ltd and Techna Group S.r.l. All rights reserved.

Keywords: Mulberry-like ZnO particles; Microwave hydrothermal method; Formation mechanism; Antibacterial property

1. Introduction

As an important semiconductor, ZnO has wide band gap energy (3.37 eV) and large binding energy (60 meV) [1,2], and has become a versatile and technologically interesting material. It has attracted much attention in recent years not only because of its potential applications in optoelectronic devices [3,4], piezoelectric generators, dye-sensitized solar cells [5], biodevices [6] and photocatalysts [7,8], but also because of its various morphologies, such as nanowires [9], nanorods [10], nanotubes [11], nanowhiskers [12], and nanoflowers [13].

Among the various ZnO morphologies, spherical ZnO has great potential applications in gas sensing [14,15], drug delivery, catalysis [16], and chemical storage,as well as photoelectric and antibacterial materials [17,18]. However, large-scale uniform spherical ZnO is hard to prepare due to its fast growth rate along c -axis [19]. In previous studies, Zhang et.al [20] synthesized monodisperse porous ZnO spheres by a soluble-starch-assisted method and the obtained ZnO samples showed excellent photocatalytic activities. Fang et.al [21] reported a good route (template-directed synthetic route) for the fabrication of ZnO hollow nanospheres, and the results indicated these obtained ZnO hollow nanospheres were a wonderful platform to immobilize glucose oxidase owing to the high specific surface area and high isoelectric point. However, traditional methods for preparing ZnO usually require rigorous conditions, sophisticated instrumentation or long reaction time [22]. Therefore, finding a simple and fast method to fabricate large-scale uniform spherical ZnO is also of great importance. Moreover, there are fewer reports on the antibacterial property of the spherical ZnO, and the reports concerning the effects of ZnO with different morphologies on antibacterial activity of *C. albicans* are more rarely seen while some research has already shown that the morphology and structure of ZnO play important roles in determining the properties of the obtained material.

*Corresponding author at: College of Resources and Environment, Shaanxi University of Science and Technology, Xi'an 710021, PR China. Tel.: +86 2986168010; fax: +86 2986168012.
E-mail address: majz@sust.edu.cn (J.Z. Ma).

0272-8842/$ - see front matter © 2012 Elsevier Ltd and Techna Group S.r.l. All rights reserved.
http://dx.doi.org/10.1016/j.ceramint.2012.09.049

Herein, we reported a fast and successful fabrication of a mulberry-like ZnO particles via a simple TEA-assisted microwave hydrothermal route. The effects of different alkali sources and different amounts of TEA on the morphology of ZnO were investigated, and then the formation mechanism of mulberry-like ZnO particles is discussed. Lastly, the antibacterial property of the obtained mulberry-like ZnO particles on *Candida albicans* (*C. albicans*) was investigated compared with other morphological ZnO.

2. Experimental section

2.1. Synthesis of ZnO

All chemicals were used as received. In a typical experiment, 0.02 mol/l zinc nitrate solution ($Zn(NO_3)_2 \cdot 6H_2O$, 98%, Tianjing Hongyan Chemical Agent Company) with total solid content of 0.3 g was added to a mixture of 10 ml deionized water and 40 ml absolute ethyl alcohol (C_2H_5OH, Tianjing Hongyan Chemical Agent Company). Then 0.075 mol of triethanolamine (TEA, Tianjing Hongyan Chemical Agent Company) or equimolas of other alkalis were added into the above-mentioned solution. After 30 min stirring, the mixture was treated by ultrasonic processing for 10 min, transferred to and sealed in a 100 ml Teflon-lined autoclave, heated to 180 °C for 15 min in a Microwave Digestion Instrument with the power of 600 W (Shanghai Sineo Microwave Chemistry Technology Co. Ltd), and then cooled to room temperature. The white precipitate was filtered, and washed with deionized water and ethanol 3 times and then dried at 60 °C for 4 h.

2.2. Characterization

X-ray diffraction (XRD) measurement was carried out on a X-ray diffractrometer (Rigaku, D/max-2200, Japan) using Cu Kα radiation. The surface morphology and the structure of the obtained ZnO were examined by field emission scanning electron microscopy (FESEM) (JSM-6700F, operated at 5 kV) and a high resolution transmission electron microscope (HRTEM); JEM-3010, Electronics Corporation of Japan. Crystal structure of the sample was confirmed by using selected area electron diffraction equipped on a JEM-3010 high resolution transmission electron microscope.

2.3. Antibacterial testing

C. albicans culture was kindly provided by Xi'an Microorganism Research Institution. The antibacterial activity of mulberry-like ZnO particles was evaluated by examining the growth density and numbers of bacterial colony with the traditional plating methods. First, bacterial inoculum (0.5 MF units) was diluted to 1:200 ($\sim 5 \times 10^5$ CFU/ml) using PBS buffer solution. Then the obtained bacterial suspension (5 ml) was introduced into a 10 ml centrifuge tube with 50 mg ZnO. The tube was kept vibrating on a Water Bathing Constant Temperature Vibrator (model: SHZ-A, Shanghai Pudong Physical Photon Instrument Company) at 150 rpm for 24 h at room temperature. Then, 1 ml mixture of the bacteria and ZnO was transferred into an agar plate and incubated in static condition at 37 °C and 90% relative air humidity for 48 h. Finally, the growth of bacteria was observed. Inhibition rates can be calculated using the following equation, where N_0 is the number of *C. albicans* without the treatment of ZnO and N_t is the number of *C. albicans* treated by ZnO for 24 h

$$\text{Inhibition rates} = \frac{N_0 - N_t}{N_0} \times 100\% \qquad (1-1)$$

In order to assess the antibacterial property of mulberry-like ZnO particles, corresponding bacterial suspensions without ZnO power and with other morphological ZnO were used as a positive control.

3. Results and discussion

3.1. Morphology and structure

Fig. 1a displays the X-ray diffraction (XRD) pattern of the obtained ZnO structures. All the diffraction peaks of XRD pattern could be indexed to the pure hexagonal wurtzite ZnO structure with calculated lattice constants of $a=0.325$ nm and $c=0.521$ nm. Because no diffraction peaks were observed from other impurities in the XRD pattern, it was concluded that pure hexagonal-phase ZnO structures were synthesized through this fast and simple microwave irradiation method. Fig. 1b shows the general morphology of the obtained ZnO. The morphology of spheres was almost 100%. Bulk quantities of ZnO products were uniform in shape and had a similar size. The diameter of ZnO spheres was about 150 nm. High magnification SEM image showed that the obtained ZnO was uniform in size and mulberry-like in shape. It was composed of many nanoparticles (Fig. 1c). Fig. 1d shows the TEM image of bulk quantities of ZnO, which further demonstrated the results of SEM images, that large-scale uniform mulberry-like ZnO particles were obtained. A typical TEM image of one mulberry-like ZnO particle is shown in Fig. 1e. Clearly the morphology of the sample was in accordance with the SEM result. Careful TEM observation in Fig. 1e showed that the surface of mulberry-like ZnO particles is formed by dozens of granular layers. Each layer was constructed by many nanoparticles with the diameter of about 5 nm.The HRTEM image in Fig. 1f confirmed the high crystallinity of the ZnO spheres and gave a lattice fringe of about 0.245 nm, which corresponds to the distance between the (101) planes in the ZnO crystal lattice. SAED pattern taken from the border of mulberry-like ZnO particles is shown in the inset, which further confirmed that the diffraction spots correspond to polycrystal hexagonal wurtzite ZnO structure.

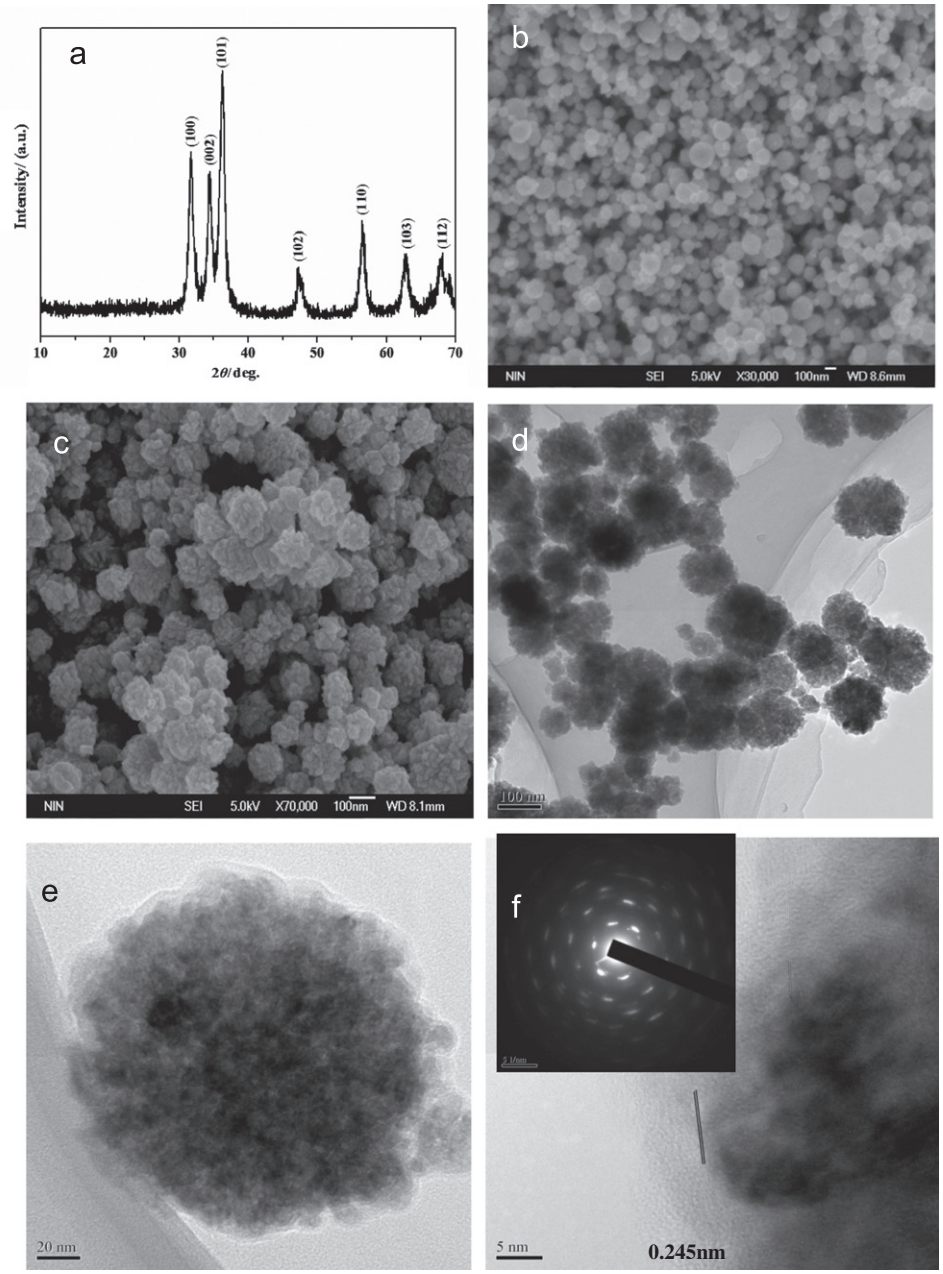

Fig. 1. (a) XRD pattern of the synthesized ZnO; (b) SEM image of the prepared ZnO (× 30,000); (c) SEM image of the prepared ZnO (× 70,000); (d) TEM image of the obtained ZnO; (e) TEM image of a single ZnO; and (f) HRTEM image of the prepared ZnO.

3.2. Formation mechanism of mulberry-like ZnO particles

The controlled experiments of microwave-assisted hydrothermal process and without TEA, instead of TEA and with different amounts of TEA were carried out to confirm the effects of TEA on the morphology of the ZnO samples. The formation mechanism of such ZnO was then investigated to judge the possible extent of this synthesis route.

Fig. 2 shows the X-ray diffraction (XRD) patterns of prepared ZnO powders with, without TEA and with equimolar NaOH and hexamethylene tetramine (HMTA) while the reaction temperature and the reaction time were still 180 °C and 15 min, respectively. It had been found that the XRD patterns of all samples identified hexagonal or wurtzite structure ZnO in accordance with the JCPDS (36-1451) as depicted in Fig. 2. The sharpness of the peaks indicated that the product was well crystallized, and no peaks belonging to the impurities were observed in the patterns. The crystallite sizes of ZnO prepared with difference alkaline sources could be calculated according to the Scherrer equation $D=(k\lambda/\beta_{hkl}\cos\theta)$, where D is the thickness of (hkl) crystal plane, λ is the wavelength of the incident X-ray (1.5406 Å for Cu Kα), k is a constant equal to 0.93, β_{hkl} is the peak width at half-maximum intensity, and h is the peak position [23]. The (101) plane was selected to calculate the average crystallite sizes. And the

estimated crystallite sizes of ZnO prepared with and without TEA and with equimolar NaOH and hexamethylene tetramine (HMTA) were 47.8 ± 2, 15.2 ± 2, 39.1 ± 2 and 30.9 ± 2 nm, respectively. These results indicated that adding TEA could restrain the growth of ZnO particles effectively and the smaller size ZnO was obtained. However, the calculated sizes were smaller than the SEM and TEM observed results. This was due to the different test principles among them. SEM and TEM results showed the grain size instead of the crystallite size of the obtained particles.

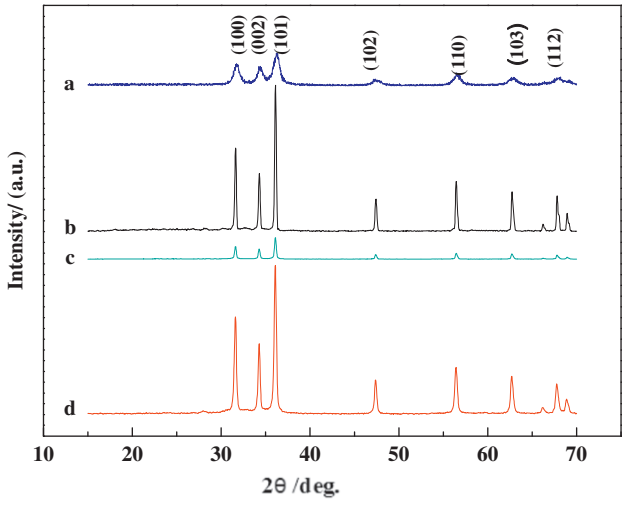

Fig. 2. XRD pattern of the synthesized ZnO (a) with TEA (b) without TEA (c) with equimolar NaOH and (d) with equimolar hexamethylene tetramine.

Fig. 3 shows the SEM images of ZnO samples prepared with different alkali sources, the other conditions being the same. The assembled ZnO with hexagonal structure was synthesized without TEA (Fig. 3b), compared with mulberry-like ZnO particles in Fig. 3a. When NaOH was used as the alkaline source, the assembled ZnO with hexagonal structure was transformed into flower-like ZnO composed of some tightly aggregated nanoneedles with an average diameter of 100 nm, but no mulberry-like ZnO particles were obtained (Fig. 3c). In the case of using equimolar HMTA instead of TEA, some rectangle and smaller ZnO particles were prepared (Fig. 3d). This was probably due to the different pH of the reaction solutions. As can be seen from Table 1, the pH value of reaction solutions containing different equimolar alkalis follows the order NaOH(>14) > TEA(9.74) > HTEA(6.74). As we know, OH^- plays a crucial role in controlling the growth of the different crystal faces owing to the formation of the $Zn(OH)_n$ complex, resulting in faster growth rate along (0 0 1) face. The higher pH, the more OH^- was. When HTMA was used, the existing OH^- would led ZnO seeds to grow along the (001) face to form some longer rectangle ZnO while the formation of smaller ZnO particles with

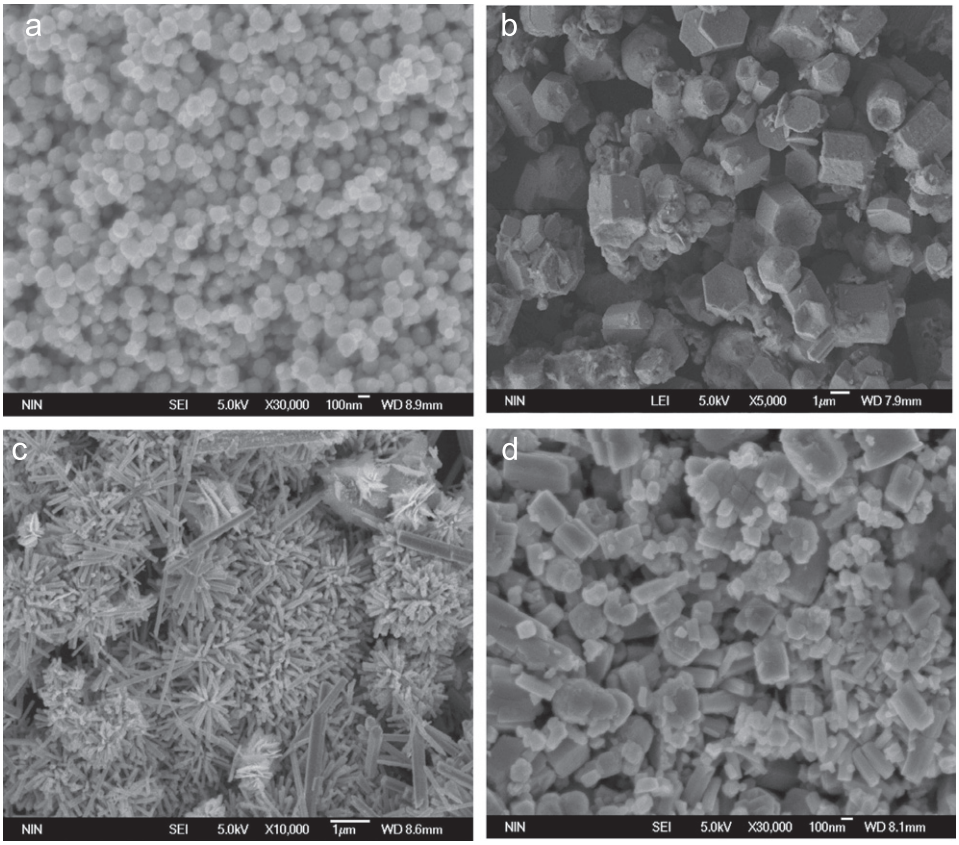

Fig. 3. SEM images of ZnO prepared (a) with TEA (b) without TEA (c) with equimolar NaOH and (d) with equimolar HMTA.

Table 1
pH value of the reaction solutions with different alkalis.

Different types of alkalis	Content (mol)	pH value of the reaction solution
None	0	4.34
HTMA	0.075	6.71
TEA	0.075	9.74
NaOH	0.075	> 14

HTMA as the alkali source might be due to the limitation of OH^- concentration. When NaOH was used, the large number of OH^- also promoted the growth of ZnO along *C*-axis. Moreover, the alkalinity of this reaction solution was stronger. It was hard to form ZnO nuclei due to the fast dissolution of ZnO crystal nucleus in the strong alkali conditions. Therefore, it should increase the critical nucleus size to improve the system stability. So needle-like ZnO gathered together and flower-like ZnO was

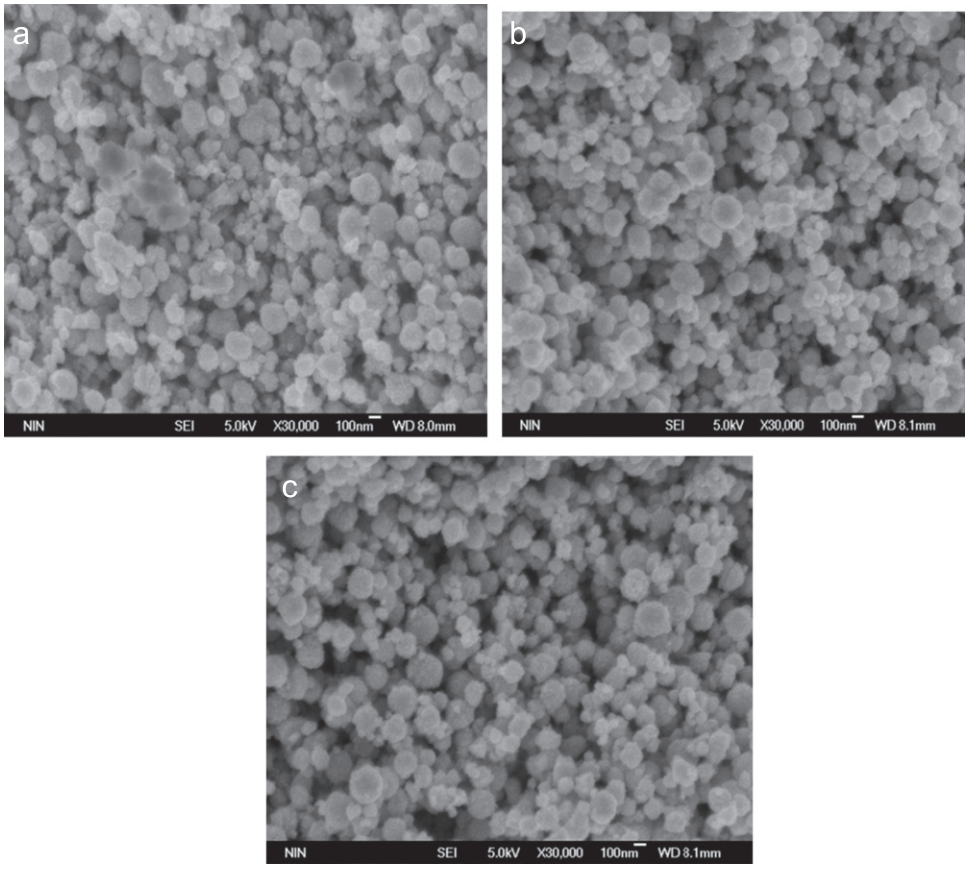

Fig. 4. SEM images of ZnO prepared with TEA: (a) 0.06 mol, (b) 0.045 mol and (c) 0.03 mol.

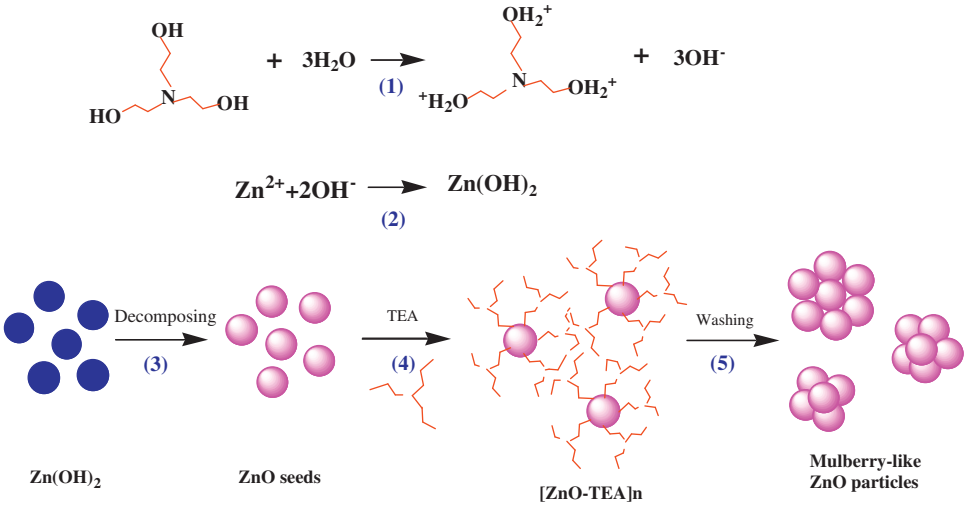

Fig. 5. Formation process of mulberry-like ZnO spheres.

produced. The formation mechanism of the mulberry-like ZnO particles with TEA as the alkali source was completely different from that using of NaOH and HTMA. And it would be discussed later.

With further changing of the mole of TEA to 0.06 mol, 0.045 mol and even 0.03 mol, mulberry-like ZnO particles could also be obtained (Fig. 4). However, the size of mulberry-like ZnO particles changed a little with different amounts of TEA. In the case of a high TEA concentration, large-scale mulberry-like ZnO particles with uniform size were obtained, while with the reduction of TEA, some larger size and irregular ZnO appeared and the sizes of mulberry-like ZnO particles were different.

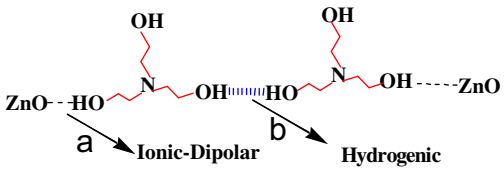

Fig. 6. Bonding formation of (a) ZnO and TEA; and (b) TEA and TEA.

The above results indicate that TEA provides incentives to change the shape of ZnO and prepare the mulberry-like ZnO particles. Due to the steric effect of three CH_2CH_2OH groups in the structure of TEA, a thick layer of organic molecules could be formed on the surface of the initially formed powders [24], which could possibly prevent the agglomeration or coagulation of particles and retard the growth of ZnO crystal along c-axis [25].

The reaction process for the preparation of mulberry-like ZnO particles can be illustrated as follows: in this process, TEA was not only the alkali source, but also the organic template [26]. The N atom in triethanolamine could be combined with protons to form a certain amount of OH^-, which could adjust the pH value of reaction system to that of a weak base, as shown in Step 1 of Fig. 5. Therefore, the initial growth unit $Zn(OH)_2$ was obtained with the reaction of Zn^{2+} and OH^- (Step 2 of Fig. 5). Then ZnO seeds were formed with the decomposition of $Zn(OH)_2$ when hydrothermally treated at elevated temperatures and under autogenous pressure (Step 3 of Fig. 5). However, in the TEA-assisted hydrothermal process, the formed ZnO seeds were attracted to some of the TEA

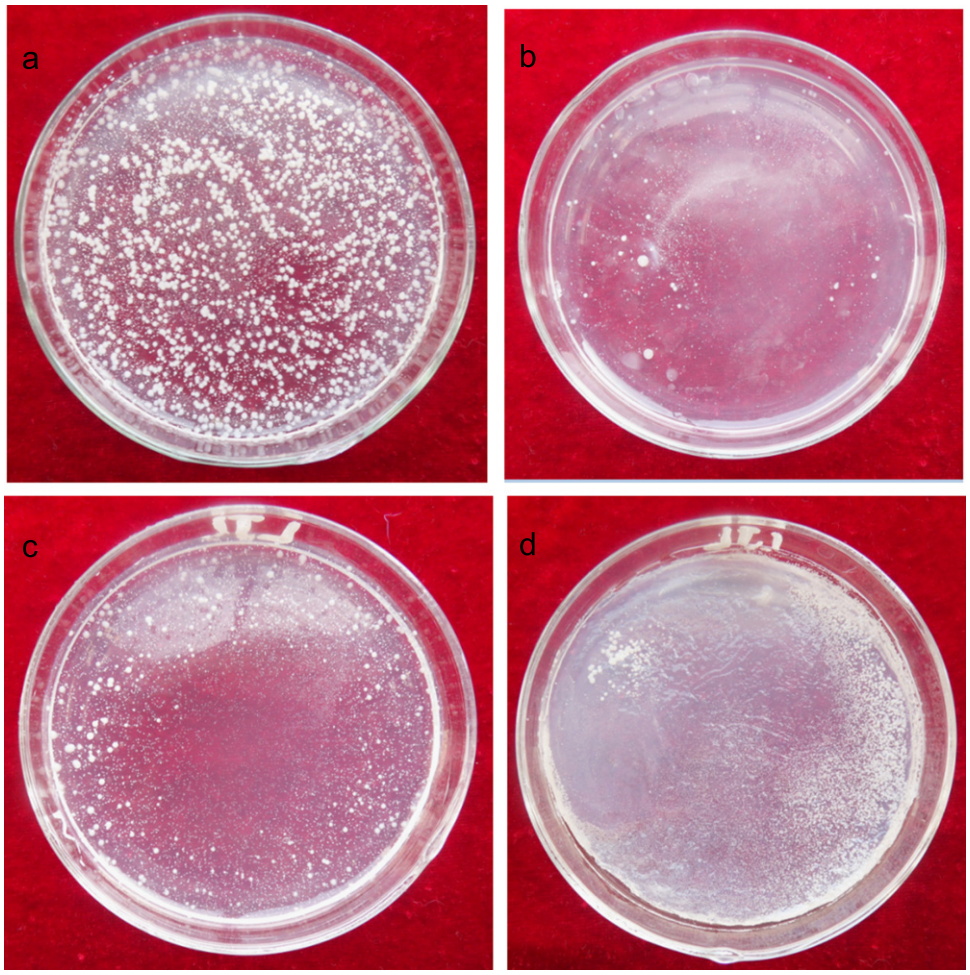

Fig. 7. Growth of *Candida albicans* (a) without the treatment of ZnO; (b) with the treatment of mulberry-like ZnO spheres; (c) with the treatment of sheet-like ZnO; and (d) with the treatment of flower-like ZnO.

chains to form TEA ligands ($[ZnO–TEA]_n$) due to the ionic-dipolar interaction (Fig. 6) between the hydrogen atoms in the polymer and the oxygen in the ZnO (Step 4 of Fig. 5). There formed TEA ligands had the ability to selectively adsorb on some specific crystal planes and then restrained the anisotropic growth of ZnO crystallites. Lastly, mulberry-like ZnO particles grew with the association of the ZnO seeds because some of the TEA chains were attracted to each other by hydrogen-bonding forces (Fig. 6). Mulberry-like ZnO particles were finally obtained after washing and removing the residual organic material (Step 5 of Fig. 5).

3.3. Antibacterial properties

Fig. 7 shows the growth of *C. albicans* without the treatment of ZnO, treated by ZnO and that with different morphologies. Compared with the other three treated ones, numerous white spots (*C. albicans* bacterial colony) were visible to the naked eye in the plate without the treatment of ZnO (Fig. 7). The inhibition rates of the three different morphological ZnO were 90% (mulberry-like ZnO particles), 85% (sheet-like ZnO),and 50% (flower-like ZnO). The mulberry-like ZnO particles showed the strongest antimicrobial activity among the tested ZnO. This may be because with the weight and concentration of ZnO suspensions being the same, small size mulberry-like ZnO particles could diffuse and adhere to the surface of bacterial cell membrane more easily, which would lead to denaturation of membrane proteins and change the permeability of membrane, further destroying bacterial cell membrane structure. Moreover, the smaller size ZnO could also permeate into the bacterial cell and combine with intracellular DNA and RNA molecules to block the genome replication. Thus mulberry-like ZnO particles were expected to have more effective antibacterial activity compared to larger size ZnO.

4. Conclusion

In conclusion, the present TEA-assisted microwave hydrothermal process is a simple and fast method to synthesize large-scale uniform mulberry-like ZnO particles. The experimental results demonstrated that the mulberry-like ZnO particles were about 150 nm in diameter with high crystallinity and composed of self-assembled nanoparticles. TEA was of great importance in the formation process of mulberry-like ZnO particles because it was both the alkali source and the organic template. Mulberry-like ZnO particles exhibited stronger antibacterial property on *C. albicans* than sheet-like and flower-like ZnO. This TEA-assisted microwave hydrothermal method can probably be employed to produce other semiconductors with novel morphologies for various potential applications and to gain a fundamental understanding of the functioning of ZnO as an antibacterial agent.

Acknowledgements

This investigation was supported by International Science and Technology Cooperation Program of China (2011DFA43490), National Natural Science Foundation of China (51073091, 21006061), The Fok Ying-Tong Education Foundation (131108) and Graduate Innovation Fund of Shaanxi University of Science and Technology.

References

[1] Y.X. Wang, X.Y. Li, N. Wang, X. Quan, Y.Y. Chen, Controllable synthesis of ZnO nanoflowers and their morphology-dependent photocatalytic activities, Separation and Purification Technology 62 (2008) 727–732.
[2] Z.W. Deng, M. Chen, G.X. Gu, L.M. Wu, A facile method to fabricate ZnO hollow spheres and their photocatalytic property, Journal of Physical Chemistry B 112 (2008) 16–22.
[3] J. Liu, Z. Guo, F.L. Meng, Novel single-crystalline hierarchical structured ZnO nanorods fabricated via a wet-chemical route: combined high gas sensing performance with enhanced optical poperties, Crystal Growth & Design 9 (2009) 1716–1722.
[4] S. Suwanboon, P. Amornpitoksuk, Preparation and characterization of nanocrystalline La-doped ZnO powders through a mechanical milling and their optical properties, Ceramics International 37 (2011) 3515–3521.
[5] M. Giannouli, F. Spiliopoulou, Effects of the morphology of nanostructured ZnO films on the efficiency of dye-sensitized solar cells, Renewable. Energy. 41 (2012) 115–122.
[6] X.S. Tang, E. Shi, G. Choo, L. Li, J. Ding, J.M. Xue, Synthesis of ZnO nanoparticles with tunable emission colors and their cell labeling applications, Chemistry of Materials American Chemical Society 22 (2010) 3383–3388.
[7] K.D. Bhatte, P. Tambade, S. Fujita, M. Arai, B.M. Bhanage, Microwave-assisted additive free synthesis of nanocrystalline zinc oxide, Powder Technology 203 (2010) 415–418.
[8] J.C. Wang, P. Liu, X.Z. Fu, Z.H. Li, W. Han, X.X. Wang, Relationship between oxygen defects and the photocatalytic property of ZnO nanocrystals in Nafion membranes, Langmuir journal 25 (2009) 1218–1223.
[9] Y. Qin, R. Yang, Z.L. Wang, Growth of horizonatal ZnO nanowire arrays on any substrate, Journal of Physical Chemistry C 112 (2008) 18734–18736.
[10] S.K. Panda, A. Dev, S. Chaudhuri, Fabrication and luminescent properties of c-axis oriented ZnO–ZnS core–shell and ZnS nanorod arrays by sulfidation of aligned ZnO nanorod arrays, Journal of Physical Chemistry C 111 (2007) 5039–5043.
[11] D.W. Chu, Y. Masuda, T. Ohji, K. Kato, Formation and photocatalytic application of ZnO nanotubes using aqueous solution, Langmuir 26 (2010) 2811–2815.
[12] H.L. Lu, X.J. Yu, Z.H. Zeng, D.L. Chen, K. Bao, L.W. Zhang, H.L. Wang, DC-field-induced synthesis of ZnO nanowhiskers in water-in-oil microemulsions, Ceramics International 37 (2011) 287–292.
[13] P. Amornpitoksuk, S. Suwanboon, S. Sangkanu, A. Sukhoom, N. Muensit, J. Baltrusaitis, Synthesis, characterization, photocatalytic and antibacterial activities of Ag-doped ZnO powders modified with a diblock copolymer, Powder Technology 219 (2012) 158–164.
[14] K.H. Lee, C.H. Park, K. Lee, T. Ha, J.H. Kim, J. Yun, Semi-transparent organic/inorganic hybrid photo-detector using entacene/ZnO diode connected to pentacene transistor, Organic Electronics 12 (2011) 1103–1107.
[15] J. Gong, Y.H. Li, X.S. Chai, Z.H. Hu, Y.L. Deng, UV-light-activated ZnO fibers for organic gas sensing at room temperature, Journal Of Physical Chemistry C 114 (2010) 1293–1298.

[16] N. Vatansever, S. Polat, Effect of zinc oxide type on ageing properties of Styrene Butadiene Rubber compounds, Materials & Design 31 (2010) 1533–1539.
[17] R.K. Dutta, P.K. Sharma, R. Bhargava, N. Kumar, Differential susceptibility of *Escherichia coli* Cells toward transition metal-doped and matrix-embedded ZnO nanoparticles, Journal of Physical Chemistry B 114 (2010) 5594–5599.
[18] R. Tankhiwale, S.K. Bajpai, Preparation, characterization and antibacterial applications of ZnO-nanoparticles coated polyethylene films for food packaging, Colloids and Surfaces., B: Biointerfaces 90 (2012) 16–20.
[19] Q.Z. Wu, X. Chen, P. Zhang, Y.C. Han, X.M. Chen, Amino acid-assisted synthesis of ZnO hierarchical architectures and their novel photocatalytic activities, Crystal Growth & Design 8 (2008) 3010–3018.
[20] G. Zhang, X. Shen, Y.Q. Yang, Facile synthesis of monodisperse porous ZnO spheres by asoluble starch-assisted method and their photocatalytic activity, Journal of Physical Chemistry 115 (2011) 7145–7152C 115 (2011) 7145–7152.
[21] B. Fang, C.H. Zhang, G.F. Wang, M.F. Wang, Y.L. Ji, A glucose oxidase immobilization platform for glucose biosensor using ZnO hollow nanospheres, Sensors and Actuators B: Chemical 155 (2011) 304–310.
[22] S. Anas, R.V. Mangalaraja, S. Ananthakumar, Studies on the evolution of ZnO morphologies in a thermohydrolysis technique and evaluation of their functional properties, Journal of Hazardous Materials 175 (2010) 889–895.
[23] A.K. Zak, W.H. Majid, H.Z. Wangc, R..Yousefi, et al., Sonochemical synthesis of hierarchical ZnO nanostructures, Ultrasonics. Sonochemistry. 20 (2013) 395–400.
[24] C.H. Lu, Y.C. Lai, R.B. Kale, Influence of alkaline sources on the structural and morphological properties of hydrothermally derived zinc oxide powders, Journal of Alloys and Compounds 477 (2009) 523–528.
[25] K. Thongsuriwong, P. Amornpitoksuk, S. Suwanboon., The effect of aminoalcohols (MEA, DEA and TEA) on morphological control of nanocrystalline ZnO powders and its optical properties, Journal of Physics and Chemistry of Solids 71 (2010) 730–734.
[26] R. Razali, A.K. Zak, W.H. Abd, M. Darroudi, Solvothermal synthesis of microsphere ZnO nanostructures in DEA media, Ceramics International 37 (2011) 3657–3663.